Energy Harvesting from Variation in Blood Pressure through Deformation of Arterial Wall using Electro-magneto-hydrodynamics

A. Pfenniger[*,1], V.M. Koch[2], A. Stahel[2] and R. Vogel[1]
[1]ARTORG Cardiovascular Engineering, University of Bern, Bern, Switzerland, [2]Bern University of Applied Sciences, Engineering and Information Technology, Biel, Switzerland
*Corresponding author: Murtenstrasse 31, CH-3010 Bern, alois.pfenniger@artorg.unibe.ch

Abstract: The present project aims at modelling a generator that harvests energy from the variation in blood pressure by exploiting the motion of the arterial wall between the diastolic and systolic phase of the cardiac cycle. The concept is to use a highly electrically conductive fluid, which is driven by the motion of the arterial wall within a separate compartment outside the artery. A constant magnetic field is applied to a part of this compartment, which allows converting the fluid's motion into electrical energy based on the principle of electro-magneto-hydrodynamics. The simulation encompasses fluid-structure interactions as well as magneto- and electrostatics and takes advantage of the multiphysics capabilities of COMSOL. The setup of the simulation allows parametric studies of the geometry.

Keywords: Energy harvesting, electro-magneto-hydrodynamics, fluid-structure interactions, electro-magnetic induction.

1. Introduction

Human energy harvesting has gained much interest in the last decade, since it opens new perspectives in terms of long-term power supply for medical implants that remain in the body for many years. Several energy sources can be considered in the human body. One of them is the cardiovascular system, with the advantage that the energy is provided continuously.

Electro-magneto-hydrodynamics (EMHD) is a phenomenon that occurs when an electrically conductive fluid (ECF) is flowing through a magnetic field. An electrical field is induced, which is perpendicular to the direction of flow and to the magnetic field.

Electro-magnetic flow measurement was the first application that used the phenomenon of EMHD. Interestingly blood was among the first fluids to be measured with this technique [1].

With regards to power generation, EMHD has been used mainly in relation with plasma generators [2,3,4]. More recently, new fields of application have emerged, like energy generation for unmanned undersea vehicles [5] or human kinematical energy harvesting from a wristwatch [6]. In this project, the use of EMHD in relation with the deformation of arteries is studied.

To model the setup of interest, the following parameters were defined:

- An artery with inner diameter of 10 mm, wall thickness of 1 mm and length of 20 mm is considered. Young's modulus for the arterial wall was taken as 5e5 Pa [7]. Poisson's ratio was set to 0.4 [8].
- The generator consists of a compartment containing the ECF and wrapped around the artery, an array of four tiny tubes connected distal to that compartment, and a flexible membrane distal to the tubes (Figure 1).
- The flexible membrane ensures that a volume of ECF can pass through the tiny tubes during systole. This membrane acts as a spring to push back the ECF during diastole.
- Permanent magnets are arranged between the tubes, such that a high magnetic flux density is achieved perpendicular to the tubes' axes.
- The gradient of blood pressure was considered negligible over the 20 mm length of the artery. Only the time dependence of the pressure pulse was considered. The Navier-Stokes equations were therefore not solved within the arterial lumen. The pressure was applied directly on the arterial wall.

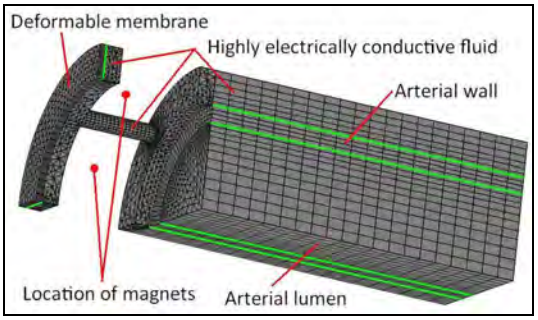

Figure 1. Geometry of generator (1/4 is represented, but only 1/8 was simulated to benefit from symmetry).

2. Methods

The pressure pulse applied to the artery was adapted from [9] and extended in order to model the complete heart cycle [7]. The period for one cycle was set to 0.9 s, leading to approximately 67 bpm. The diastolic and systolic pressures were set to 80 mmHg and 120 mmHg, respectively. The pressure pulse's waveform is given by the following equation (in [Pa]):

$$p(t) = 10666 + 2667 \cdot \begin{cases} 0.5 + 0.5 \cdot \cos(10 \cdot \pi \cdot (t - 0.1)), & 0 < t \le 0.1 \\ 1.5 - 0.5 \cdot \cos(10 \cdot \pi \cdot (t - 0.5)), & 0.1 < t \le 0.3 \\ 0.5 + 0.5 \cdot \cos(5/3 \cdot \pi \cdot (t - 0.3)), & 0.3 < t \le 0.9 \end{cases}$$

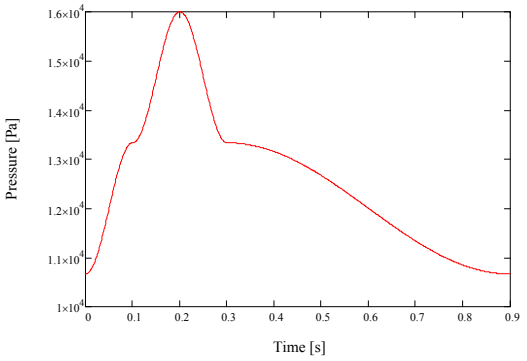

Figure 2. Pressure pulse as function of time.

The dimensions at diastolic pressure were taken to model the artery. Initial stress conditions were applied to the arterial wall to account for the stress resulting from the diastolic pressure.

First approximation for initial normal stresses σ_x, σ_y and σ_z were obtained by Laplace's law. σ_x and σ_y were evaluated by Laplace's law for a tube, whereas σ_z was evaluated by Laplace's law for a sphere [7]. The drawback of this approach is the impossibility to resolve the stress in its different spatial components. Rather, it computes a mean stress over the cross-section of the arterial wall. Furthermore, only normal stresses can be estimated with this method. A stationary simulation of the initial state (artery under diastolic pressure) showed that with the initial stress distribution obtained from Laplace's law, the artery deviated from its initial shape. In a second step, the initial stress conditions (normal and shear stresses) were evaluated by a separate simulation. The artery was placed in a totally relaxed state, i.e. without any pressure applied to it, translating to a smaller inner diameter. The deformation under diastolic pressure was then simulated. Polynomial regressions as function of the radial and angular positions were performed to better resolve the spatial distribution of the stress components:

$$\sigma_x = A \cdot \cos(\varphi - \pi/4) \cdot \sin(\varphi - \pi/4) + B$$

$$\sigma_y = A \cdot \cos(\varphi + \pi/4) \cdot \sin(\varphi + \pi/4) + B$$

$$\sigma_z = A$$

$$\sigma_{xy} = C \cdot x \cdot y$$

$$\sigma_{yz} = \sigma_{xz} = 0$$

where

$$A = -22.2e6 \cdot r + 181e3$$

$$B = -14.2e12 \cdot r^3 + 235e9 \cdot r^2 - 1.30e9 \cdot r + 2.41e6$$

$$C = -669e12 \cdot r^2 + 8.82e12 \cdot r - 30.2e9$$

$$\varphi = atan2(y,x)$$

$$r = \sqrt{x^2 + y^2}$$

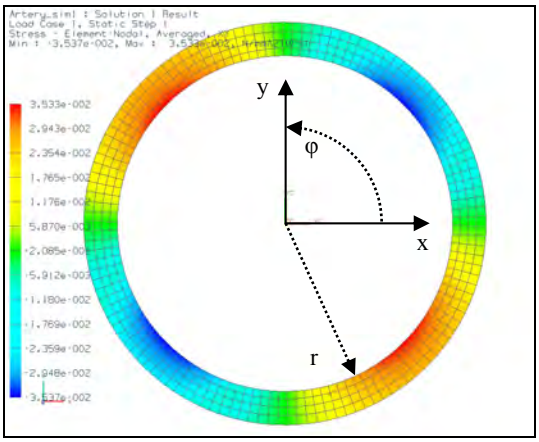

Figure 3. Stationary simulation of the artery under diastolic pressure to evaluate initial stress conditions.

With this improved initial stress distribution, the artery under diastolic pressure did not deviate from its initial shape by more than 2 μm.

To model the proposed setup, five application modes were used:

- Incompressible Navier-Stokes (ns)
- Moving Mesh (ale)
- Structural Mechanics, Solid, Stress-Strain (smsld)
- AC/DC, Magnetostatics, No Current (emnc)
- AC/DC, Conductive Media DC (emdc)

In the following sections, the different application modes and their relevant settings are explained.

2.1 Incompressible Navier-Stokes

The incompressible Navier-Stokes equations (conservation of mass and momentum) were solved for the domains containing the ECF:

$$\nabla \cdot \vec{u} = 0$$

$$\rho \cdot \frac{\partial \vec{u}}{\partial t} + \rho(\vec{u} \cdot \nabla)\vec{u} = -\nabla p + \mu \nabla^2 \vec{u} + \vec{F} \qquad (1)$$

where u is the velocity field of the fluid [m/s], ρ is the fluid's density [kg/m^3] and μ is the fluid's dynamic viscosity [Pa·s]. F is a volume force field that acts on the fluid [N]. No-slip boundary conditions were set for the fixed walls, whereas moving walls were defined at the interface between the ECF and the arterial wall and between the ECF and the membrane. Symmetry conditions were set at the symmetry planes.

2.2 Moving Mesh

To ensure that the domain containing the ECF adapts to the shape of the arterial wall and the membrane, a moving mesh was implemented for all the domains. The normal mesh displacement was constrained at the symmetry planes.

2.3 Solid, Stress-Strain

The arterial wall was modelled using an elastic material. Viscoelastic effects, known to produce a hysteresis loop in the stress-strain diagram, which lead to energetic losses, are therefore not taken into account.

The pressure increase in the ECF, due to deformation of the arterial wall, was applied as surface load on the arterial wall and on the membrane to obtain proper two-way coupling.

2.4 Magnetostatics, No Current

The distribution of the magnetic field was computed once at the beginning of the simulation. Possible perturbations due to the electric current flowing through the generator were neglected.

2.5 Conductive Media DC

Ions moving in a magnetic field experience a force, the Lorentz force, which is expressed as:

$$\vec{F}_L = q \cdot (\vec{u} \times \vec{B})$$

where q is the charge [C] and B is the magnetic flux density [T]. This force tends to separate the positively from the negatively charged ions, leading to Coulomb forces between the ions, which generate an electrical field:

$$\vec{F}_C = q \cdot \vec{E}$$

Equilibrium is reached when both forces are equal (but in opposite direction), which allows defining the electric field as function of the flow velocity and the magnetic flux density:

$$\vec{F}_C = -\vec{F}_L \quad \Rightarrow \quad \vec{E} = -\vec{u} \times \vec{B} \qquad (2)$$

Ohm's law is expressed as:

$$\vec{J} = \sigma \cdot (\vec{E} + \vec{u} \times \vec{B}) \qquad (3)$$

where E is bounded due to the load resistor (Figure 4). σ is the ECF's electric conductivity [S/m].

Poisson's equation for the scalar electric potential φ is expressed as:

$$\vec{E} = -\nabla \varphi \qquad (4)$$

Introducing (4) in (3), and using charge conservation $\nabla \cdot \vec{J} = 0$, the equation can be rewritten as:

$$-\nabla \cdot (\sigma \cdot \nabla \varphi - \sigma \cdot \vec{u} \times \vec{B}) = 0$$

For the source in the open loop, one can state $\vec{E} = -\vec{u} \times \vec{B}$ (cf. (2)) and therefore $\vec{J} = \vec{0}$ (cf. (3)). To ensure optimal power transfer between source and load, the resistor has to match the internal resistance of the generator. In that case, $\vec{E} = \frac{-\vec{u} \times \vec{B}}{2}$, and $\vec{J} = \sigma \cdot \frac{\vec{u} \times \vec{B}}{2}$.

The load resistor was modelled using COMSOL's Spice Circuit Editor. The generated power was computed as:

$$P = U \cdot I$$

where U is the voltage measured across the load resistor and I is the current through the resistor.

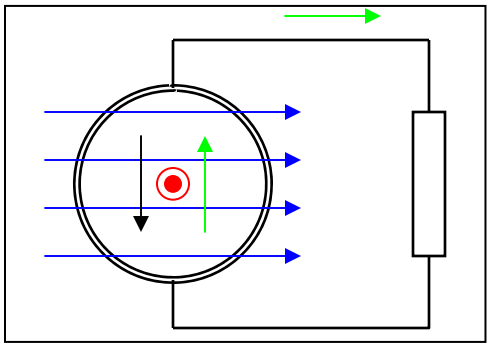

Figure 4. Schematic representation of generator (cross-section) and load resistor. Arrows: blue = B; red = u; green = J; black = E

Obviously, if power is consumed in the load (and lost in the source due to its internal resistance), a force must counteract the ECF's motion to ensure energy conservation. This force is produced by the current flow through the magnetic field across the generator:

$$\vec{F} = \vec{J} \times \vec{B} \qquad (5)$$

This force field was implemented in the Navier-Stokes equation – last term on the right of (1) – to model two-way coupling between the two application modes [10].

3. Solver sequence

The following sequence was defined to solve the model for a given geometry:

- First, the internal resistance of the generator is computed by applying a known voltage.
- Second, the magnetic field distribution is simulated and stored for further computations.
- Third, the stationary situation of arterial wall and membrane are computed to find initial conditions to the time dependent problem.
- Finally, the time dependant simulation is run.

The whole model is built in Matlab®, which makes a parametric study very convenient. A loop can be defined for a given geometrical dimension to be evaluated.

4. Results

The generator presented in this section has an arbitrary geometry. Realistic values were chosen for the free parameters.

Instantaneous and mean power (14.6 nW) in the load resistor are displayed below. Taking into account that only 1/8 of the geometry was modelled, the mean power of the whole system would reach 117 nW.

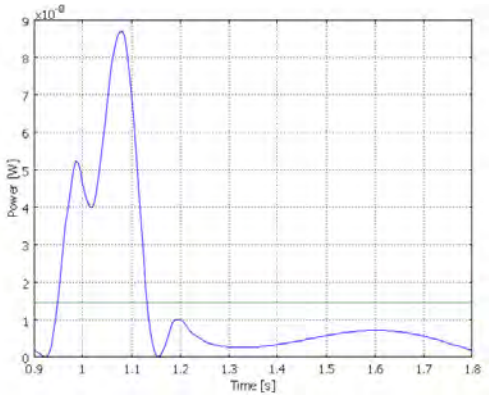

Figure 5. Instantaneous (blue) and mean (green) power in the load resistor as function of time.

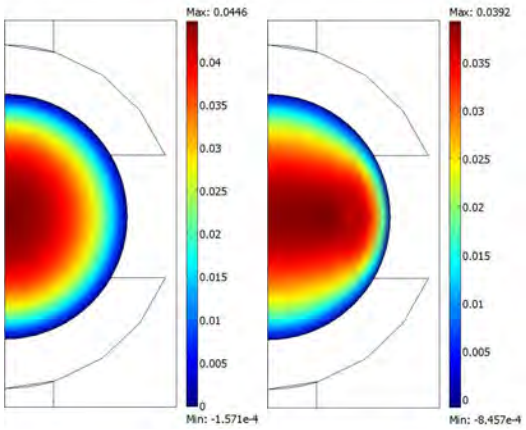

Figure 6. Flow velocity through a section of the tube, displayed at half of the tube's length (left: no decelerating force; right: decelerating force).

Comparing the situation with and without decelerating force (cf. (5)), it can be noted that the flow pattern is deformed (Figure 6). Furthermore, the maximum velocity is decreased by 12%.

The maximum radial deformation of the arterial wall reaches 224 µm and 28 µm without and with the generator around the artery. This is a drastic reduction of deformation amplitude. Improved conditions can be expected when a good balance between deformation amplitude and output power is found (no deformation at all means no flow through the generator, thus no

generated power; too large deformation means a lot of elastic energy stored in the arterial wall, thus little power is generated).

To validate the simulation, the influence of the load resistor and the decelerating force can be analysed. The table below contains the maximal radial deformation (MRD) of the arterial wall as well as the strain energy (SE) stored in it during systole. Two different load resistors where simulated: a 10 kΩ resistor that mimics an infinitely high load and a resistor matching the internal resistance of the generator.

	No decelerating force	**Decelerating force**	
		R_{load} = 10k	$R_{load} = R_{int}$
MRD	27.82 μm	27.76 μm	27.71 μm
SE	10.1420 μJ	10.1147 μJ	10.0853 μJ
ΔSE	-	29.4 nJ	

A diminution of the deformation amplitude already occurs when modelling the decelerating force with a 10 kΩ resistor. This is explained by the fact that "short-circuit" currents occur within the ECF due to the inhomogeneity of the induced electrical field [1]. In Figure 6, the flow pattern on the right shows the case for a load resistor matching the internal resistance of the generator. With a 10 kΩ resistor, a similar pattern can already be observed.

When switching from 10 kΩ to a resistor matching the internal resistance, the MRD decreases further. Computing the difference in strain energy between the two resistors leads to 29.4 nJ. The mean power in the load resistor was found before to be 14.6 nW, which corresponds to an energy of 13.2 nJ during 0.9 s. The same amount of energy is also lost in the generator, resulting in a total energy of 26.4 nJ. The error between the generated energy (26.4nJ) and the energy difference in the arterial wall (29.4nJ) is 11%, which is surprisingly small taking into account the strong transients in the pressure pulse and the multi-way couplings between the different physics.

5. Discussion

The different comparisons presented in the previous section show that all the effects that were modelled behave correctly: selecting the load resistor such that the current through the generator is maximised decreases the amplitude of the arterial wall's deformation. Furthermore, energy conservation is ensured within an error of 11%. With this setup, other configurations can be examined.

The work by [11] showed that an elliptical cross-section is preferable over a circular one with regard to sensor's sensitivity for an electro-magnetic flowmeter. The same methodology could also be implemented in the current study to increase output power.

6. References

1. J.A. Shercliff, *The Theory of Electromagnetic Flow-Measurement*, p. 3, Cambridge University Press, Cambridge (1962)
2. H. Branover, *Magnetohydrodynamic Flow in Ducts*, Israel Universities Press, Jerusalem (1978)
3. R.J. Rosa, *Magnetohydrodynamic Energy Conversion*, Hemisphere Publishing, Washington (1987)
4. H.K. Messerle, *Magnetohydrodynamic Electrical Power Generation*, Wiley, Chichester (1995)
5. S.R. Snarski et al., Device for electro-magnetohydrodynamic (EMHD) energy harvesting, *Edward M. Proceedings of the SPIE*, **Vol. 5417**, pp. 147-161 (2004)
6. D. Jia et al., Harvesting human kinematical energy based on liquid metal magnetohydrodynamics, *Physics Letters A*, **Vol. 373**, pp. 1305-1309 (2009)
7. N. Westerhof et al., *Snapshots of Hemodynamics*, pp. 31,39,106. Springer Science, New York (2005)
8. C. Lees et al., Poisson's Ratio in Skin, *Bio-Medical Materials and Engineering*, **Vol. 1**, pp. 19-23 (1991)
9. P. Vasava et al., Pulsatile Blood Flow Simulations in Aortic Arch: Effects of Blood Pressure and the Geometry of Arch on Wall Shear Stress, *IFMBE Proceedings*, **Vol. 22**, pp. 1926-1929 (2009)
10. W.B.J. Zimmerman, *Multiphysics Modelling with Finite Element Methods*, pp. 375-391, World Scientific Publishing Company, Singapore (2006)
11. J. Krause, G. Stange, Design and Optimisation of a Magnetic-inductive Flow Sensor with Elliptical Cross-Section, *Excerpt from the Proceedings of the Comsol Users Conference 2006,* Frankfurt (2006)